Preferential Localization of a Vesicular Monoamine Transporter to Dense Core Vesicles in PC12 Cells

Yongjian Liu,* Erik S. Schweitzer,‡ Melissa J. Nirenberg,‖ Virginia M. Pickel,‖ Christopher J. Evans,§ and Robert H. Edwards*

Departments of *Neurology and Biological Chemistry,‡Anatomy & Cell Biology, and §Psychiatry; Molecular Biology Institute, UCLA School of Medicine, Los Angeles, California 90024-1769; and ‖Department of Neurology and Neuroscience, Cornell University Medical College, New York 10021

Abstract. Neurons and endocrine cells have two types of secretory vesicle that undergo regulated exocytosis. Large dense core vesicles (LDCVs) store neural peptides whereas small clear synaptic vesicles store classical neurotransmitters such as acetylcholine, γ-aminobutyric acid (GABA), glycine, and glutamate. However, monoamines differ from other classical transmitters and have been reported to appear in both LDCVs and smaller vesicles. To localize the transporter that packages monoamines into secretory vesicles, we have raised antibodies to a COOH-terminal sequence from the vesicular amine transporter expressed in the adrenal gland (VMAT1). Like synaptic vesicle proteins, the transporter occurs in endosomes of transfected CHO cells, accounting for the observed vesicular transport activity. In rat pheochromocytoma PC12 cells, the transporter occurs principally in LDCVs by both immunofluorescence and density gradient centrifugation. Synaptic-like microvesicles in PC12 cells contain relatively little VMAT1. The results appear to account for the storage of monoamines by LDCVs in the adrenal medulla and indicate that VMAT1 provides a novel membrane protein marker unique to LDCVs.

NEUROTRANSMITTERS are stored in secretory vesicles that undergo regulated exocytosis. Peptide transmitters enter the secretory compartment by co-translational translocation of a precursor protein into the lumen of the endoplasmic reticulum and subsequently undergo processing and packaging into mature vesicles (de Camilli and Jahn, 1990; Trimble et al., 1991; Kelly, 1991). In contrast, the synthesis of classical transmitters such as acetylcholine, γ-aminobutyric acid (GABA),[1] glycine, glutamate, and the biogenic amines occurs in the cytoplasm. These transmitters also appear in the cytoplasm after removal from the synapse by specific plasma membrane reuptake systems (Amara and Kuhar, 1993). Thus, classical transmitters require specific transport from the cytoplasm for packaging into secretory vesicles. In addition, the storage of neural peptides and classical transmitters occurs in distinct vesicle populations.

Address all correspondence to R. H. Edwards, Department of Neurology, UCLA School of Medicine, 710 Westwood Blvd., Los Angeles, CA 90024-1769. Ph.: (310) 206-7672. Fax: (310) 206-2502.

1. *Abbreviations used in this paper*: CGAT, chromaffin granule amine transporter; DBH, dopamine β-hydroxylase; DFP, diisopropylfluorophosphate; GABA, γ-aminobutyric acid; HBS, Hepes-buffered saline; KLH, keyhole limpet hemocyanin; LDCV, large dense core vesicles; MBS, *m*-maleimidobenzoyl *N*-hydroxysuccinimide; MPP^+, *N*-methyl-4-phenylpyridinium; mppres, Mpp^+ resistant; NGS, normal goat serum; PAM, peptidylglycine α-amidating monooxygenase; VMAT1, vesicular amine transporter.

Neural cells store peptide transmitters in large dense core vesicles (LDCVs), the functional equivalent of the secretory granules in which endocrine cells store peptide hormones (Kelly, 1991; Trimble et al., 1991). These granules range in size from 40 to over 100 nm and have a characteristic dense core in electron micrographs, presumably due to their protein content. LDCVs also have a relatively diffuse distribution in the cytoplasm. They appear in nerve terminals but not at the same high density as classical synaptic vesicles; they also occur in the cell body and dendrites. In contrast, neurons store classical transmitters such as acetylcholine, GABA, glycine, and glutamate in small clear synaptic vesicles of 40–50 nm (Sudhof and Jahn, 1991; Edwards, 1992). Typical synaptic vesicles cluster in large numbers at the nerve terminal, in close proximity to the presynaptic membrane. In addition to these differences in structure and localization, large dense core vesicles and synaptic vesicles also differ in function. Exocytosis from LDCVs occurs with a longer latency after stimulation than exocytosis from synaptic vesicles (de Camilli and Jahn, 1990). The observed differences in rate of release presumably account for the relatively prolonged action of peptides as neural modulators and the more rapid action of classical neurotransmitters in direct signaling. In addition, high frequency stimulation favors release from LDCVs relative to synaptic vesicles (Andersson et al., 1982). Differential sensitivity to α-latrotoxin (Matteoli et al., 1988), and intracellular calcium (Rane et al.,

1987; Martin and Magistretti, 1989) further indicates that exocytosis from the two types of vesicle involves distinct mechanisms. Thus, the storage of peptide and classical transmitters in different vesicular compartments has clear implications for the regulation of their release and for their role in synaptic transmission. Since the packaging of classical transmitters into vesicles requires transport from the cytoplasm, the selective packaging of specific transmitters into different types of vesicles depends on the expression of specific transport activities by these different vesicles.

Previous studies have identified at least four distinct vesicular transport activities: one for the biogenic amines, a second for acetylcholine, another for GABA and glycine and a fourth for glutamate (Sudhof and Jahn, 1991; Edwards, 1992). The availability of bovine adrenal chromaffin granules and their robust transport activity have made the vesicular transport of monoamines a prototype for vesicular neurotransmitter transport. Studies using this preparation have shown that vesicular amine transport depends on a pH gradient generated by the vesicular H^+-ATPase (Kanner and Schuldiner, 1987; Johnson, 1988). The transporter exchanges two lumenal protons for a cytoplasmic amine. Recent studies have shown that the vesicular transporters for other classical transmitters depend on different aspects of the same H^+-electrochemical gradient (Anderson et al., 1982; Maycox et al., 1988; Hell et al., 1990). However, classical transmitters do not all appear to be stored in the same vesicular compartment. Typical small synaptic vesicles express specific transport activities for acetylcholine, GABA, glycine, and glutamate, consistent with storage in this compartment (Burger et al., 1989). On the other hand, cells in the adrenal medulla store monoamines with neural peptides in large dense core chromaffin granules (Johnson, 1988). In the central nervous system, neurons store monoamines in small vesicles that may contain a dense core depending on the method of fixation (Smith, 1972; Thureson-Klein, 1983). Thus, the storage of monoamines appears to differ from that of other classical transmitters and presumably reflects the differential sorting of vesicular transport proteins.

Using selection in the neurotoxin *N*-methyl-4-phenylpyridinium (MPP^+), we have recently cloned a cDNA encoding the chromaffin granule amine transporter (CGAT) or vesicular amine transporter (VMAT1) (Liu et al., 1992*b*; Erickson et al., 1992). The transporter protects against this toxin by sequestering it in intracellular vesicles, away from its primary site of action in mitochondria (Liu et al., 1992*a*). The sequence predicts a protein with twelve transmembrane domains and weak homology to several bacterial antibiotic resistance transporters (Liu et al., 1992*b*). We have now used the amino acid sequence deduced from this cDNA to design a synthetic peptide, produce polyclonal antisera to the transporter and determine its intracellular location. The results indicate expression of the transporter in endocytic vesicles of CHO fibroblasts and preferential expression in LDCVs of neuro-endocrine PC12 cells.

Material and Methods

Cell Culture

CHO cells were maintained in Ham's F-12 medium with 5% FCS and rat pheochromocytoma PC12 cells in modified DME with 10% horse serum and 5% FCS. All cultures were kept at 37°C in 5% CO_2 and all media contained penicillin and streptomycin.

CHO cells were co-transfected as previously described (Liu et al., 1992*a*) with 10 μg of the VMAT1 cDNA in the plasmid expression vector CDM8 and 1 μg of the selectable marker Rous sarcoma virus-neomycin (RSV-neo) per 10 cm plate. After initial selection in 400 μg/ml G418 for 2 wk, the cells were selected again in 1 mM MPP^+ for at least 3 wk. MPP^+-resistant (mpp^{res}) cells were maintained in the absence of the toxin for at least 1 wk before study.

To label the dense core granules with [^{3}H]norepinephrine, PC12 cells were incubated in standard medium containing 5 μCi [^{3}H]noradrenaline (Amersham Corp., Arlington Heights, IL)/25 ml for at least 6 h before cell fractionation.

Peptide Synthesis and Antibody Production

The peptide CGENSDDPSSGE was synthesized manually and coupled to keyhole limpet hemocyanin (KLH) through the NH_2-terminal cysteine using *m*-maleimidobenzoyl *N*-hydroxysuccinimide ester (MBS). For the primary inoculation, 150 μg of the conjugated peptide was emulsified in complete Freund's adjuvant and injected intradermally into adult female rabbits (Harlow and Lane, 1988). Antibody production was boosted 4 wk later by the subcutaneous injection of 100 μg conjugated peptide emulsified in incomplete Freund's adjuvant. After 12 d, the animals were bled through an ear vein. The antibody titer following the first boost was then measured using the unconjugated peptide in a solid-phase ELISA (Harlow and Lane, 1988). Animals making anti-peptide antibodies were then boosted further with 100 μg of conjugated peptide at 4-wk intervals, with serum collected 2 wk after each boost. The anti-peptide antibodies were purified on a peptide affinity column of epoxy-activated Sepharose 6B (Pharmacia Fine Chemicals, Piscataway, NJ). For adsorption, the antibody was diluted 1:100 in 500 μl 0.1% Tween-20/PBS, 0.5 mg peptide added, the mixture incubated overnight at 4°C, and then diluted further in the same solution for immunostaining.

Immunostaining

For immunocytochemistry, cells cultured overnight in a 24-well plate were fixed in 4% paraformaldehyde/0.1 M PBS, pH 7.2, permeabilized in 0.2% Triton X-100/PBS for 15 min and blocked with 5% nonfat dry milk in PBS for 30 min at room temperature. The cells were then incubated for 60 min with the primary antibody diluted 1:1,000–1:5,000 in 1% nonfat dry milk/PBS and washed three times in PBS, each for 5 min. Incubation in a secondary biotinylated anti-rabbit antibody (Vector Labs, Burlingame, CA) was also carried out for 30 min, followed by three 5-min washes in PBS. The complexes were visualized using avidin-biotin conjugated to alkaline phosphatase (Vector Labs).

For immunocytochemistry of the adrenal gland, adult, male Sprague-Dawley rats were anesthetized with sodium pentobarbital (50 mg/kg i.p.) and perfused through the ascending aorta with 4% paraformaldehyde/0.1 M sodium phosphate, pH 7.2. The adrenal gland was then dissected, postfixed again in the same solution for an additional hour at room temperature, incubated in 30% sucrose at 4°C overnight, frozen, sectioned at 10 μm, and the tissue collected on gelatin-coated slides for immunocytochemistry as described above.

For immunofluorescence, both CHO and PC12 cells were grown on glass coverslips to 60–80% confluence and processed as described (Schweitzer and Paddock, 1990). PC12 cells were treated with 10 ng/ml NGF in medium containing serum for four days before staining. The cells were then fixed as described above, permeabilized in 0.1% Triton X-100/Hepes-buffered saline (HBS), and then incubated with anti-peptide antibody diluted 1:1,000 in 1% normal goat serum (NGS)/HBS. After washing in HBS, the cells were incubated at room temperature with goat anti-rabbit antibody conjugated to fluorescein diluted 1:100 in 1% NGS/HBS, washed again, and visualized with epifluorescence. Double staining with WGA conjugated to Texas red and monoclonal antibodies to tubulin, secretogranin I, and synaptophysin was carried out simultaneously. The mouse antibodies were visualized by incubation with a biotinylated sheep anti-mouse antibody followed by streptavidin-Texas red (Amersham Corp.).

To identify transferrin receptors, the CHO cells were pre-incubated in serum-free medium at 37°C for 60 min to remove endogenous transferrin, incubated with 20 μg/ml human transferrin conjugated to Texas red (Molecular Probes, Eugene, OR) for an additional 30 min, rinsed quickly in cold medium without transferrin, and then fixed and the cells examined under epifluorescence.

Membrane Preparation and Cell Fractionation

Cell membranes were prepared as described previously (Liu et al., 1992*b*). Briefly, cells rinsed twice in cold HBS containing 5 mM MgEGTA were detached from the substrate by scraping in HBS with EGTA supplemented by 1 μg/ml leupeptin and 0.2 mM diisopropylfluoro-phosphate (DFP). The cells were then homogenized by repeated passage through a ball-bearing device (European Molecular Biology Labs, Heidelberg, Germany) at a clearance of 10 μm. The nuclei and other cell debris were pelleted by centrifugation at 750 *g* for 5 min. To prepare membranes, the supernatant was centrifuged again at 35,000 rpm in a Beckman SW50.1 for 45 min at 4°C and the pellet resuspended in either HBS or electrophoresis sample buffer (67.5 mM Tris, pH 6.8, 3% SDS, 10% glycerol, 5% 2-mercaptoethanol).

For cell fractionation by equilibrium sedimentation, the postnuclear supernatant was layered onto a linear 0.6–1.6 M sucrose gradient in 10 mM Hepes for sedimentation at 30,000 rpm for 6 h in an SW41 rotor (Beckman Instruments, Palo Alto, CA) at 4°C. Fractions were collected from the bottom of the tube and stored at −70°C. The protein content was monitored using the Bradford assay (Bio-Rad Laboratories, Richmond, CA) and the radioactivity of fractions from cells pre-loaded with [^{3}H]norepinephrine measured in Ecolume (ICN Biomedicals, Irvine, CA) using a Beckman 3800 scintillation counter.

For velocity sedimentation through glycerol, the post-nuclear supernatant was centrifuged in a SW50.1 (Beckman Instruments) at 48,000 rpm for 1 h at 4°C through 5–25% glycerol in HBS containing 1 mM EGTA (Clift-O'Grady et al., 1990) and the fractions processed as described above. For metrizamide gradients, the postnuclear supernatant from cells disrupted in 0.32 M sucrose/4 mM Hepes, pH 7.4/0.5 mM EDTA (SH buffer) was centrifuged for 2.25 h at 55,000 rpm in a 70.1 Ti rotor (Beckman Instruments) through 10–23% metrizamide over a cushion of 35% metrizamide, with the 10 and 23% stock solutions of metrizamide prepared by dilution of 35% metrizamide with SH buffer (Green et al., 1994), and the fractions processed in the same way as the other gradients.

Gel Electrophoresis and Western Blot Analysis

Postnuclear supernatants and aliquots from fractions of the sucrose gradient were diluted in 2× sample buffer and separated by electrophoresis through 10% SDS–polyacrylamide containing 6 M urea. The resulting gels were transferred to nitrocellulose (BA-S NC; Schleicher & Schuell) using a semi-dry electrotransfer apparatus (E&K Scientific Products Inc., Saratoga, CA). Aliquots from the metrizamide and glycerol gradients were immobilized on nitrocellulose dot blots. The filters were then blocked in 0.1% Tween-20/PBS (TBS) containing 5% nonfat dry milk, incubated in primary antibody for 60 min in TBS with 1% nonfat dry milk, washed three times in TBS and then incubated with secondary antibody conjugated to peroxidase. The immune complexes were visualized by chemiluminescence (Amersham Corp.) and quantitated by densitometry.

Metabolic Labeling and Immunoprecipitation

CHO and PC12 cells at moderately high density were metabolically labeled with [^{35}S]cysteine and methionine (Translabel; ICN Biomedicals) at 0.25 mCi/ml in cysteine- and methionine-free medium supplemented by 1% dialyzed FCS. When indicated, tunicamycin was added at 20 ng/ml to inhibit N-linked glycosylation. After labeling for 6 to 12 h, the cells were rinsed with PBS, detached from the substrate by scraping in 1% sodium deoxycholate, 1% Triton X-100, 0.2% SDS, 150 mM NaCl, 50 mM Tris, pH 7.4 (RIPA buffer) containing 20 μg/ml PMSF, and the nuclear debris removed by centrifugation.

For immunoprecipitation, the resuspended cells were diluted to a final volume of 1 ml RIPA and incubated overnight at 4°C with affinity-purified anti-peptide antibody at a dilution of 1:1,000. The antigen-antibody complexes were precipitated by incubation for 4 h at 4°C with 200 μl 10% prewashed protein A sepharose (Sigma Chemical Co., St. Louis, MO) and the precipitates washed three times in RIPA (Edwards et al., 1988). The beads were then resuspended in 50 μl 2× sample buffer and 25 μl separated by electrophoresis through 10% SDS–polyacrylamide containing 6 M urea. After electrophoresis at 10–25 mA, the gels were fixed in 10% acetic acid/50% methanol for 20 min, impregnated with 1 M sodium salicylate for 20 min, dried, and exposed to film at −70°C with an enhancing screen.

N-Glycanase Digestion

For N-glycanase digestion, the immunoprecipitate obtained as described above from PC12 cells metabolically labeled with [^{35}S]cysteine and methionine was resuspended in 0.5% SDS/50 mM β-mercaptoethanol/50 mM $NaPO_4$, pH 8. 20 μg protein was then digested with 0.3 U of N-glycanase (Genzyme Corp., Boston, MA) in the presence or absence of 1.2% NP-40 at 37°C overnight, the reaction stopped by dilution in sample buffer, and the products analyzed by electrophoresis through polyacrylamide containing SDS.

Immunoisolation

Fixed *S. aureus* cells were pre-coated with: (*a*) rabbit VMAT1 anti-peptide antibody; and (*b*) rabbit anti-goat antisera as control by incubation with gentle rotation in 150 mM NaCl, 10 mM Hepes, pH 7.4, 1 mM EGTA, 1 mM $MgCl_2$, 1% BSA (buffer A) for 2 h at 4°C. The cells were then washed three times in buffer A and incubated with postnuclear supernatants containing ~30,000 dpm from PC12 cells pre-labeled with [^{3}H]norepinephrine as described above. For immunoisolation with the SV2 antibody, *Staphylococcus aureus* cells were pre-coated first with a rabbit anti-mouse antibody; then with (*c*) mouse SV2 monoclonal antibody; and (*d*) normal mouse serum as control. After incubation of the cell extracts with the pre-coated beads for 2 h at 4°C, the mixtures were precipitated by centrifugation at 1,000 *g* and the radioactivity in the supernatant determined by liquid scintillation counting. Subtraction of the radioactivity in the supernatant from the total radioactivity yielded the radioactivity in the immunoprecipitated vesicles.

Immunoelectron Microscopy

Methods for tissue preparation and immunolabeling were based on those described by Leranth and Pickel (1989). Adult male Sprague-Dawley rats (250–350 g) were anesthetized as described above with sodium pentobarbital and perfused with 40 ml heparinized saline (1,000 U/ml heparin in 0.15 M NaCl) followed by 50 ml 3.75% acrolein and then by 200 ml 2% paraformaldehyde/0.1 M sodium phosphate, pH 7.4. The adrenal glands were removed, postfixed in 3.75% acrolein for 30 min and sections cut on a vibratome at 40 μm. The sections were then incubated for 30 min in 1% sodium borohydride/0.1 M sodium phosphate, pH 7.4 to remove reactive aldehydes and rinsed repeatedly in 0.1 M sodium phosphate, pH 7.4. The sections were cryo-protected for 15 min in 25% sucrose/3.5% glycerol/0.05 M sodium phosphate, pH 7.4 and rapidly freeze-thawed in chlorodifluoromethane followed by liquid nitrogen.

Sections were incubated in anti-VMAT1 antibody diluted 1:12,000 in 0.1% BSA/0.15 M NaCl/25 mM Tris, pH 7.6, and the bound antibodies identified with an avidin–biotin complex (Hsu et al., 1981). Briefly, the sections were incubated first for 30 min in a 1:50 dilution of biotinylated goat anti-rabbit IgG in 0.1% BSA and then for 30 min in a 1:100 dilution of the peroxidase–avidin–biotin complex. The tissue was then incubated for 6 min in Tris-buffered saline containing diaminobenzidine and hydrogen peroxide to visualize the bound peroxidase.

Sections were fixed in 2% osmium tetroxide for 60 min and flat embedded in Epon 812 between two pieces of Aclar plastic. Ultrathin sections were collected from the outer surface of the plastic-embedded tissue using an RMC ultramicrotome, counterstained with lead citrate, and examined using a Phillips 201 electron microscope.

Results

Production and Characterization of VMAT1 Antibody

Although the sequence of VMAT1 indicates an extremely hydrophobic protein with 12 predicted transmembrane domains and few antigenic regions, we synthesized a 16–amino acid peptide from the relatively hydrophilic COOH terminus and added a cysteine to the NH_2 terminus of the sequence for coupling through MBS to the carrier KLH. After immunization, rabbit sera were screened for the presence of antibodies using a peptide ELISA. Animals producing antibodies to the peptide were boosted again and their sera tested further by immunostaining MPP^+ resistant CHO cells transfected with the VMAT1 cDNA (Liu et al., 1992*b*).

The antisera from one rabbit recognized the VMAT1 protein in transfected but not wild-type CHO cells (Fig. 1). The

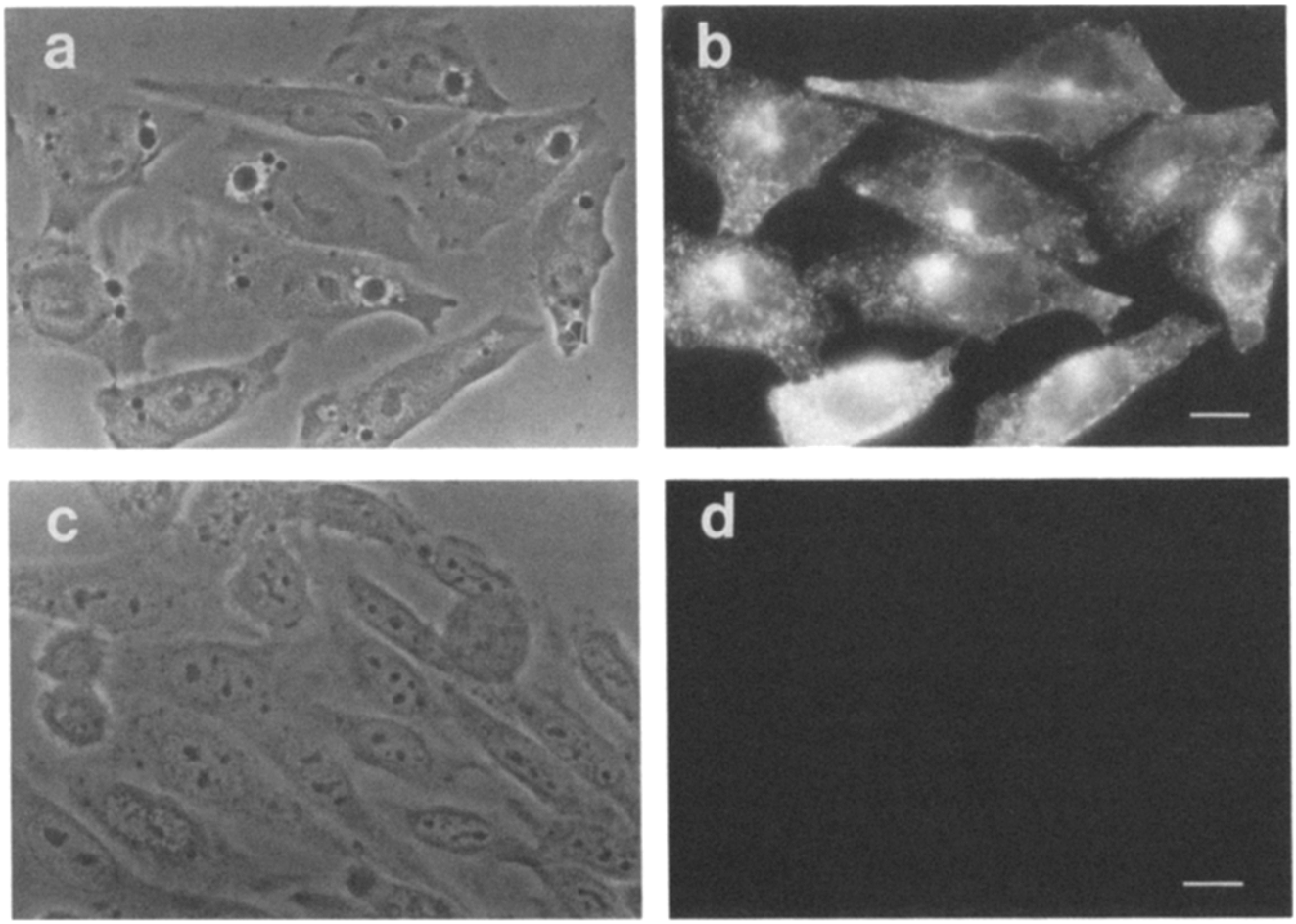

Figure 1. Immunostaining with an anti-peptide antibody shows a particulate cytoplasmic pattern of VMAT1 expression in transfected CHO fibroblasts. CHO cells transfected with the VMAT1 cDNA and selected in MPP+ (*a* and *b*) and untransfected wild-type CHO cells (*c* and *d*) were immunostained with an anti-peptide antibody to VMAT1 at a dilution of 1:2,000 and visualized by phase contrast (*a* and *c*) and epi-fluorescence (*b* and *d*). The transfected cells show a particulate pattern of cytoplasmic fluorescence very similar to that seen previously for pre-loaded dopamine (Liu et al., 1992*a*), whereas wild-type cells show no immunoreactivity. Comparison of the phase contrast and fluorescence micrographs shows that the focal concentration of fluorescence observed in transfected cells is outside of but adjacent to the nuclei. Bar, 10 μm.

perinuclear and scattered particulate cytoplasmic staining strongly resembled the distribution of intracellular dopamine observed after loading these same MPP^+-resistant cells with exogenous dopamine (Liu et al., 1992*a*). To characterize the antibody further, we tested its ability to detect VMAT1 by Western blotting (Fig. 2). Wild-type CHO cells expressed no immunoreactive protein whereas transfected MPP^+-resistant cells expressed large amounts of an ~55-kD protein and smaller but still substantial amounts of an ~95-kD protein. Rat pheochromocytoma PC12 cells, from which the VMAT1 cDNA originally derived, expressed small amounts of the 55-kD protein, and variable amounts of a higher molecular weight form of ~120 kD. In both cell types the size differed from previous work indicating a protein of ~75 kD in bovine chromaffin granules (Stern-Bach et al., 1990; Vincent and Near, 1991; Isambert et al., 1992) but the species origin of the cDNA from rat and the use of urea in the gel system may alter the electrophoretic mobility of this extremely hydrophobic protein. In addition, previous studies have concentrated on one of the two transport isoforms separated by isoelectric focusing (Stern-Bach et al., 1990). The differences in amount of VMAT1 expressed by the different cells are consistent with variations in the amount of VMAT1 mRNA previously observed in CHO transfectants and PC12 cells (Liu et al., 1992*b*). In addition, adsorption of the antibody with the peptide eliminated these immunoreactive species on Western blots (data not shown). Although the antisera had a titer of 1:1,000–1:2,000 and produced relatively low background staining in transfected cells, the antibody was further purified on a peptide affinity column (Pharmacia Biotech Inc.) and used at a dilution of 1:10,000–1:20,000.

To characterize the ability of the anti-peptide antibody to recognize VMAT1 in vivo, we have also used the antiserum to immunostain sections of the rat adrenal gland. Fig. 3 *a* shows strong staining of chromaffin cells in the adrenal medulla and no staining of cortical cells. As expected for a vesicle protein, the medullary cell immunoreactivity was principally cytoplasmic and did not include the nucleus. Adsorption with the peptide eliminated the medullary staining

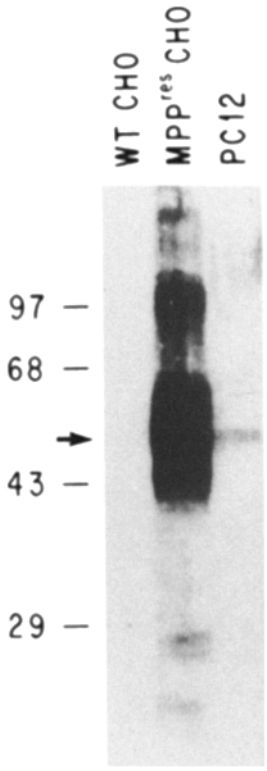

Figure 2. The anti-peptide antibody recognizes VMAT1 by Western blot analysis. 25 μg of protein from a membrane preparation of wild-type CHO cells, CHO cells stably transfected with VMAT1 and selected in MPP^+ (MPP^{res}), and wild-type PC12 cells were separated by electrophoresis through 10% polyacrylamide–SDS containing 6 M urea, blotted to nitrocellulose, stained with the anti-peptide VMAT1 antibody at a dilution of 1:2,000, and the reaction visualized by chemi-luminescence (Amersham Corp.). Transfected CHO cells contain extremely large amounts of an approximately 55-kD protein (*arrow*) as well as higher molecular weight forms whereas wild-type CHO cells contain no immunoreactive material. PC12 cells contain smaller amounts of the ~55-kD protein (*arrow*) as well as higher molecular weight forms that vary in intensity.

(Fig. 3 *b*). The origin of the cortical staining remains unclear and was occasionally but not always reduced by peptide adsorption as well.

Localization of VMAT1 to Endocytic Vesicles in Transfected CHO Cells

The transfection of cDNAs for synaptic vesicle proteins into nonneural cells has led to their localization at a number of characteristic intracellular sites. Heterologous expression of synaptophysin in CHO fibroblasts results in protein localizing to vesicles that concentrate at the microtubule organizing center; this staining co-localizes with the transferrin receptor that marks a population of recycling microvesicles (Johnston et al., 1989; Cameron et al., 1991). In contrast, the vesicle protein synaptotagmin appears at the plasma membrane when expressed in CHO cells (Feany et al., 1993). The demonstration of vesicular amine transport activity in membranes prepared from transfected CHO cells (Liu et al., 1992*b*) suggested that the transporter localizes to intracellular vesicles containing a vacuolar H^+-ATPase and so resembles the targeting of synaptophysin rather than synaptotagmin.

In MPP^+-resistant CHO cells, the particulate pattern of glyoxylic acid–induced fluorescence after loading with exogenous dopamine suggests the presence of VMAT1 in intracellular vesicles (Liu et al., 1992*a*). Immunostaining with the antibody to VMAT1 supported this impression (Fig. 4). Double-staining with an antibody to tubulin further indicated that the peri-nuclear site of protein accumulation coincides with the microtubule organizing center (Fig. 4, *b* and *c*) and double staining with WGA demonstrated substantial steady-state expression in the vicinity of the Golgi complex (Fig. 4, *e* and *f*). To determine whether the amine transporter specifically localizes to a population of recycling vesicles, we incubated the living cells with human transferrin conjugated to Texas red for 30 min and then stained the cells for the transporter. Colocalization of the tagged human transferrin with the immunoreactive transport protein strongly supported the presence of the transporter in a population of recycling vesicles (Fig. 5). Sucrose density gradients also demonstrated the coincidence of vesicles containing the transferrin receptor with those containing the amine transporter (data not shown). Thus, the heterologous expression of VMAT1 in CHO cells results in targeting of the transporter in a manner similar to that of other neuronal vesicle proteins such as synaptophysin and SV2 (Johnston et al., 1989; Cameron et al., 1991) and differs from the localization previously reported for synaptotagmin (Feany et al., 1993). The results further indicate that the vesicular amine transporter contains by itself the signals for sorting to the endocytic pathway and does not rely on association with another synaptic vesicle protein. Sorting to a population of acidic vesicles thus allows functional expression of the transporter in a nonneural cell line.

Localization of VMAT1 in PC12 Cells to Large Dense Core Vesicles

To determine the intracellular localization of VMAT1 in neuro-endocrine cells that store monoamines, we have examined the distribution of the endogenous protein expressed by PC12 cells. As noted above, the anti-VMAT1 antibody recognizes the vesicular amine transporter expressed by these cells. Further, these typically round cells can be treated with NGF to induce the formation of neural processes and so facilitate intracellular localization. Immunostaining with the antibody to VMAT1 shows predominant expression of the antigen in the ends of processes (Fig. 6), with relatively little staining in the cell bodies. To determine the relationship of this immunoreactivity to dense core granules, we have stained the same cells with an antibody to secretogranin I, a soluble protein of LDCVs, and found the same pattern of distribution in the tips of processes. Thus, VMAT1 co-localizes with secretogranin I. Since previous studies have demonstrated the differential distribution of LDCVs and SLMVs in NGF-treated PC12 cells (Schweitzer and Paddock, 1990), we performed similar double-staining with antibodies to VMAT1 and the synaptic vesicle protein synaptophysin, which appears at much higher levels in SLMVs than in dense core granules (Navone et al., 1986). In contrast to secretogranin, immunostaining of NGF-treated PC12 cells with the antibody to synaptophysin showed expression predominantly in cell bodies and to a lesser extent at the ends of processes. Staining of the same cells with the anti–VMAT1 antibody indicated a distinct pattern of distribution, with most expression in the processes. Thus, the morphologic examination of PC12 cells by light microscopy indicates expression of VMAT1 in dense core granules and suggests its relative exclusion from SLMVs.

To characterize further the subcellular distribution of VMAT1 in PC12 cells, we have also fractionated the cells by equilibrium sedimentation through sucrose density gradients (Schweitzer and Kelley, 1985). The dense core granule fraction was identified by pre-loading the cells with [^{3}H]norepinephrine (Fig. 7 *A*). An immunoblot of the fractions stained

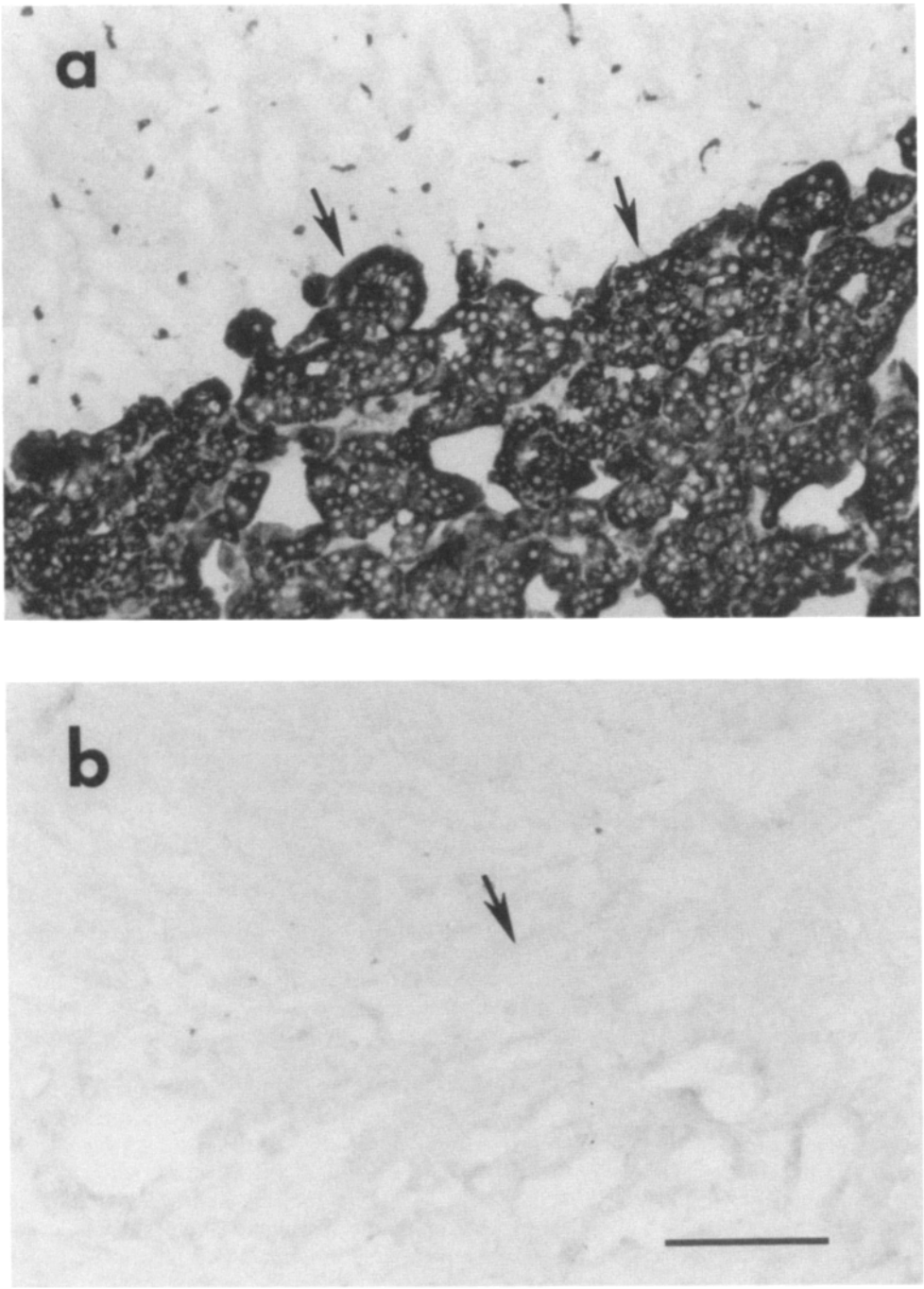

Figure 3. Adrenal medullary cells express VMAT1. Sections from the rat adrenal gland were stained with the anti-peptide antibody to VMAT1 (*a*) and with the same antibody after adsorption with the peptide used to generate it (*b*). All cells in the adrenal medulla (*arrows*) but none in the cortex react with the antibody. Adsorption with the peptide eliminates the medullary immunoreactivity entirely and reduces the punctate staining observed to varying degrees in the cortex. Bar, 150 μm.

with an antibody to secretogranin II indicated that this protein resides as expected in the heavier, dense core granules also pre-labeled with [^{3}H]norepinephrine (Fig. 7 *B*). In contrast, an antibody to synaptophysin labeled predominantly a lighter fraction of vesicles distinct from the peak of soluble protein, with variable but substantially lower levels of expression in the dense core granule fraction. The anti-peptide antibody to VMAT1 detected the 55-kD form of the protein in the peak of LDCVs centered at fraction 6. No immunoreactive protein of this size appeared in the lighter fractions. However, the immunoreactive material migrating at ~120 kD appeared in both heavy and light membrane fractions. To determine whether this material is VMAT1 or unrelated background, we immunostained another Western blot containing fractions from the gradient with a preparation of antibody that had been adsorbed with the peptide used to generate it. Pre-adsorption with the peptide abolished the staining of both the 55- and ~120-kD bands, indicating that both of these species contain VMAT1. Thus, the endogenous vesicular amine transporter expressed by PC12 cells occurs in two forms, a low molecular weight form that appears to reside exclusively in LDCVs and a higher molecular weight form that predominates in dense fractions but also occurs in lighter membranes, possibly

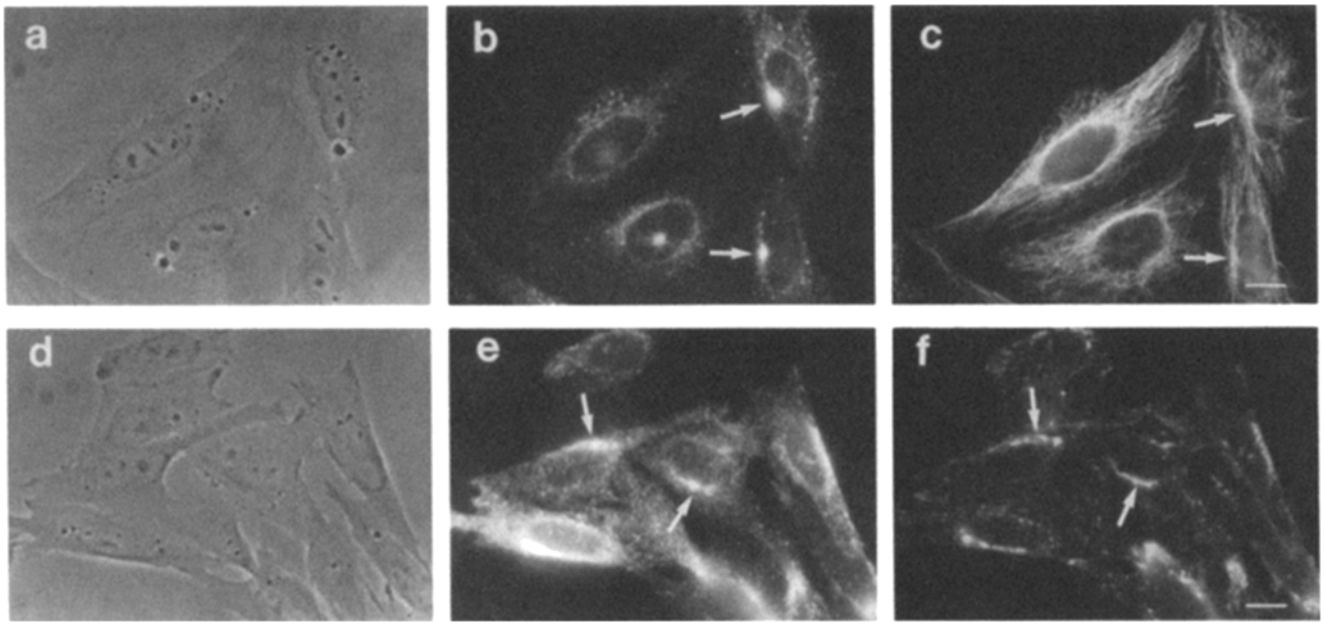

Figure 4. VMAT1 immunofluorescence in transfected CHO fibroblasts co-localizes with the microtubule-organizing center and the Golgi complex. Stable CHO transformants expressing VMAT1 were viewed by phase contrast (*a* and *d*) and immunostained with the polyclonal rabbit VMAT1 antibody (*b* and *e*), a mouse monoclonal antibody to tubulin (*c*) and WGA conjugated to Texas red (*f*). For double staining of the two sets of cells (*a–c* and *d–f*), the VMAT1 rabbit antibody was visualized with a secondary antibody conjugated to fluorescein and the mouse anti-tubulin antibody with a secondary antibody conjugated to Texas red. The strong punctate peri-nuclear VMAT1 immunoreactivity (*arrows*, *b*) co-localizes with the microtubule organizing center (*arrows*, *c*). Additional peri-nuclear VMAT1 staining (*arrows*, *e*) co-localizes with wheat germ agglutinin (*arrows*, *f*). Bar, 10 μm.

SLMVs or plasma membrane vesicles. The higher molecular weight form usually but not always (Fig. 2) predominates in PC12 cells, independent of the method of analysis (by Western blot of cell homogenates or immunoprecipitation of metabolically labeled cell extracts). However, the high molecular weight form does not simply occur as soluble protein since it had a higher density distinct from the peak of soluble protein that appeared at the top of the gradient.

Large membrane proteins, particularly those with multiple predicted transmembrane domains, have a tendency to aggregate, possibly accounting for the higher molecular weight form of VMAT1 observed in PC12 cells. However, preparation of the extracts from transfected CHO cells under the identical conditions did not yield the same species, suggesting that a modification specific to PC12 cells is responsible for this form. To characterize this modification further, we metabolically labeled both CHO and PC12 cells, immunoprecipitated VMAT1 from the postnuclear supernatant and treated the precipitates with N-glycanase to remove N-linked carbohydrate. As expected from the immunoblots, wild-type CHO cells expressed no detectable VMAT1 (Fig. 8) whereas the MPP^+-resistant CHO transformants expressed proteins of ~55 and ~95 kD. Treatment with N-glycanase reduced both of these to a species migrating at ~40 kD. The immunoprecipitate from PC12 cells also contained small amounts of a protein of ~55 kD in addition to larger amounts of the ~120-kD protein seen on immunoblots. Interestingly, treatment of this immunoprecipitate with N-glycanase resulted in increased amounts of a ~50-kD protein. This indicated that the high molecular weight form of VMAT1 expressed in PC12 cells does not represent aggregates but rather extensive N-linked carbohydrate modification. Pulse-chase studies confirm a precursor-product relationship between the two forms (Liu, Y., and R. H. Edwards, manuscript in preparation). The failure to reduce the proteins in PC12 cells to the size obtained after digestion of the proteins expressed in CHO cells further suggests either incomplete digestion or a second modification not removed by N-glycanase. The treatment of PC12 cells with tunicamycin also showed reduction of the principal species to only ~50 kD (data not shown), suggesting that a second modification is responsible. We have identified a similar high molecular weight form of the transporter in Western blots of protein extracted from the rat adrenal gland (data not shown), indicating that this modification is not unique to PC12 cells and occurs in vivo as well.

Both Endosomes and Synaptic-like Microvesicles Contain Small Amounts of VMAT1

Quantitation of immunoblots by densitometry shows that 65% VMAT1 occurs in LDCVs and 19% in lighter fractions. This preferential localization to LDCVs differs from that of other membrane proteins that occur in both compartments. In contrast to VMAT1, 42% SV2 immunoreactive protein resides in LDCVs and 49% in lighter fractions (data not shown). To localize the VMAT1 immunoreactivity that appears in lower density fractions on the sucrose gradient, we have used additional density gradients. Light vesicle fractions from the sucrose gradient may contain endosomes, SLMVs or both. To determine whether VMAT1 occurs on endosomes as well as LDCVs, we have used sedimentation

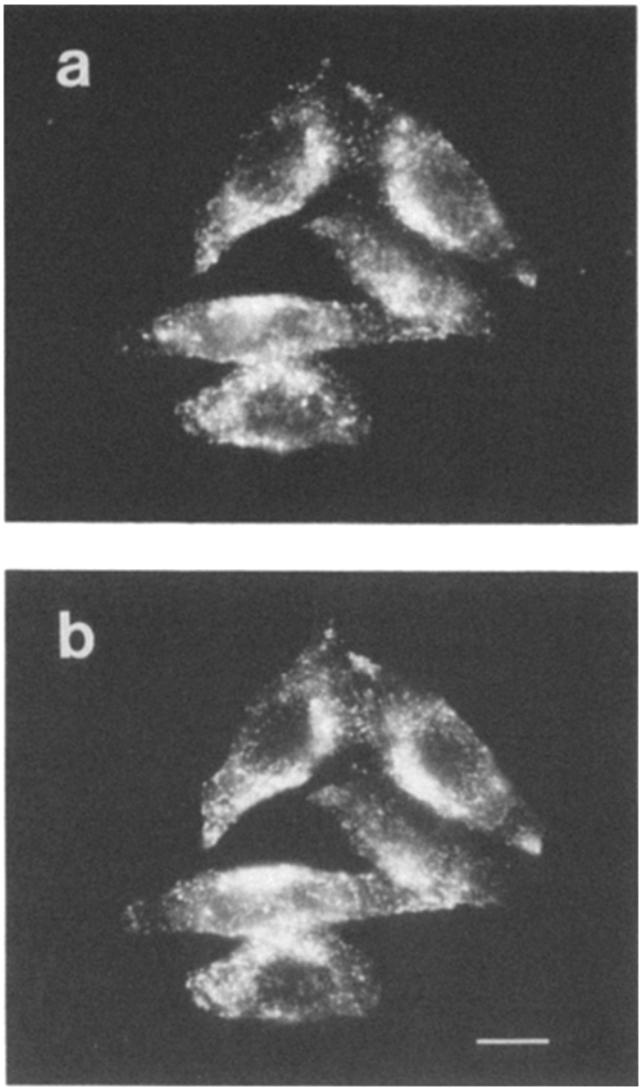

Figure 5. VMAT1 immunofluorescence co-localizes with a population of recycling endocytic vesicles. Stable CHO transformants expressing VMAT1 were pre-incubated with human transferrin conjugated to Texas red for 30 min and immunostained for VMAT1. Visualization of VMAT1 immunoreactivity with a secondary antibody conjugated to fluorescein (*a*) shows a virtually identical pattern of labeling to the transferrin receptor (*b*) as a marker of recycling endocytic vesicles. Bar, 10 μm.

through metrizamide. Fig. 9 shows that on this gradient LDCVs containing secretogranin II sedimented more rapidly than endosomal membranes containing the transferrin receptor and SLMVs expressing synaptophysin. VMAT1 appeared at both sites in the gradient, reflecting localization to the more rapidly sedimenting LDCVs and by a lighter vesicle fraction, either SLMVs or endosomes. Lighter membranes contain virtually no secretogranin II, presumably because the soluble contents of LDCVs are secreted rather than recycled.

To separate endosomes from SLMVs, we used velocity sedimentation through glycerol (Fig. 10). Using this gradient, transferrin receptor, secretogranin and pre-loaded [^{3}H]norepinephrine localized to the bottom of the gradient whereas a peak of synaptophysin was present in the middle. Thus, SLMVs do not sediment as rapidly as endosomes and LDCVs in this gradient. A fraction of VMAT1 co-sedimented with synaptophysin, indicating localization on SLMVs. The analysis of VMAT1 localization in CHO cells and the study of other vesicle proteins would predict significant targeting of VMAT1 to endosomes; these gradients are consistent with such a localization although they do not explicitly prove it.

Nonspecific monoamine uptake or uptake by a transport protein distinct from VMAT1 may mediate storage in vesicles that do not express VMAT1. To examine this possibility, we have used the antibody to VMAT1 to isolate vesicles from PC12 cells pre-incubated with [^{3}H]norepinephrine. If vesicles that do not contain VMAT1 store monoamines, we would only be able to immunoisolate a fraction of the total stored radioactivity using this antibody. As a positive control, we used the vesicle membrane protein SV2 which occurs on both LDCVs and SLMVs (Schweitzer and Kelly, 1985). The monoclonal antibody to SV2 immunoisolates all of the radiolabeled transmitter in the preloaded vesicles (Fig. 11). The VMAT1 antibody also precipitated essentially all the [^{3}H]norepinephrine contained in vesicles, excluding uptake into a distinct compartment.

Immunoelectron Microscopic Localization of VMAT1 in Chromaffin Granules

To determine the subcellular distribution of VMAT1 in vivo, we have used immunoelectron microscopy. Fig. 12 shows labeling of the rat adrenal medulla with the antibody to VMAT1 visualized with peroxidase. The antibody-labeled chromaffin granules but not the nucleus, early Golgi complex or mitochondria. At higher resolution (Fig. 13), the antibody also labeled the endoplasmic reticulum and *trans*-Golgi network. Thus, immunoreactivity for VMAT1 occurs at several sites in the secretory pathway but most prominently in the chromaffin granules, supporting the results in PC12 cells. Sympathetic nerve fibers entering the adrenal medulla contain occasional LDCVs and abundant small clear vesicles that do not react with the antibody (Fig. 13 *b*). In contrast to the sympathetic innervation of other peripheral tissues, sympathetic innervation of the adrenal gland involves direct projection of the preganglionic neuron to the target without an intervening post-ganglionic neuron. Since pre-ganglionic neurons use acetylcholine as their neurotransmitter rather than monoamines, sympathetic nerve terminals within the adrenal gland would not be expected to express a vesicular amine transporter. In addition, we have found that post-ganglionic sympathetic neurons express VMAT2 rather than VMAT1 (D. Peter, C. Sternini, N. Brecha, and R. H. Edwards, preliminary observations).

Discussion

Using an antibody raised against the COOH terminus of the vesicular amine transporter expressed in the adrenal gland, we have localized the protein in transfected CHO fibroblasts to a population of recycling endocytic vesicles. By immunofluorescence, the transporter co-localizes with recycling transferrin receptors. In addition, peri-nuclear staining co-localizes with markers for the microtubule organizing

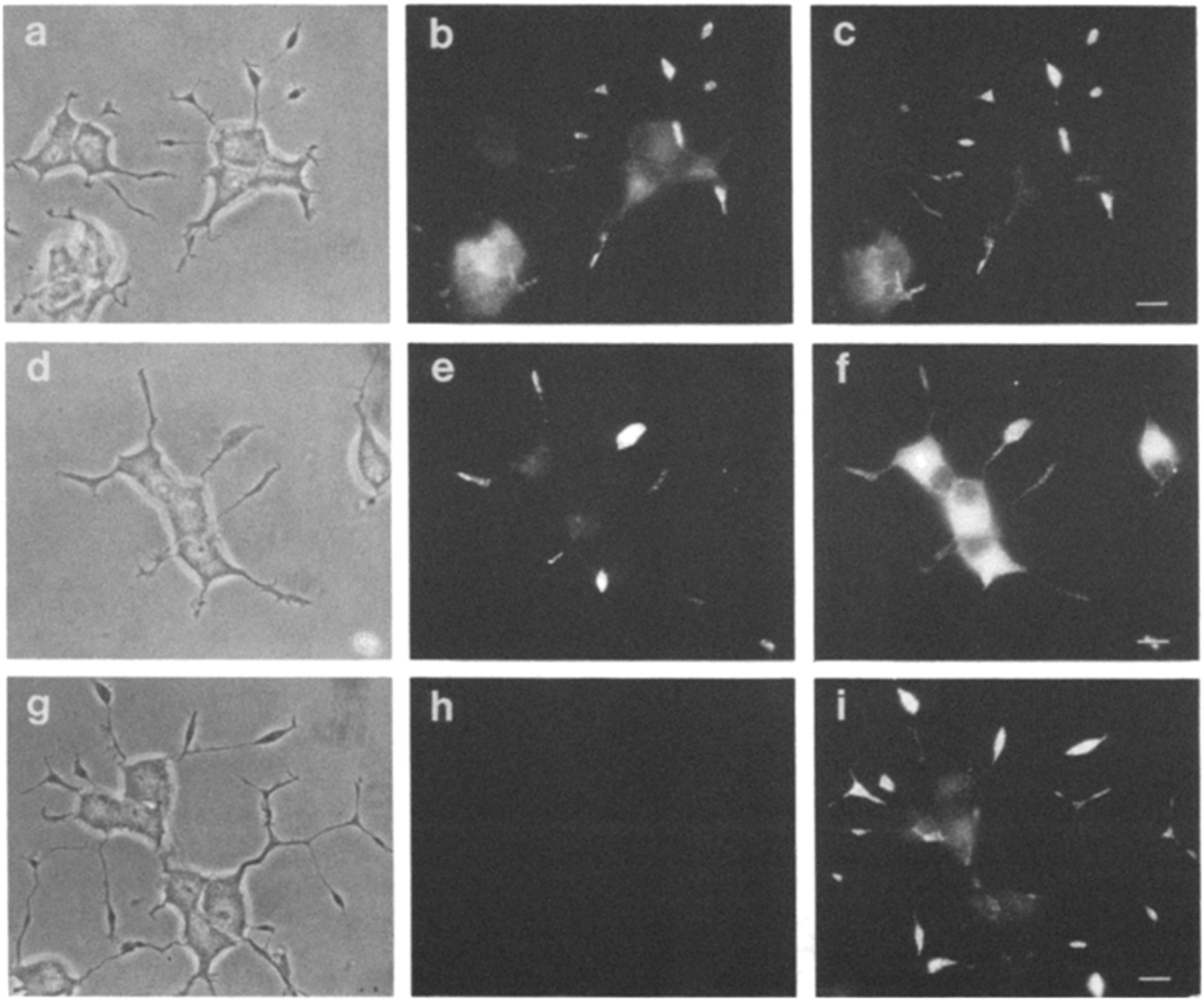

Figure 6. Endogenous VMAT1 immunofluorescence in PC12 cells co-localizes with LDCVs rather than SLMVs. PC12 cells were treated with NGF (10 ng/ml) for 4 d before staining. Three sets of cells (*a–c*, *d–f* and *g–i*) were viewed by phase contrast (*a*, *d*, and *g*), stained with the rabbit VMAT1 antibody (*b* and *e*) and the same antibody after adsorption with the peptide used to generate it (*h*) and the reactions visualized with a secondary antibody conjugated to fluorescein. The same cells were double-stained with a mouse monoclonal antibody to secretogranin I (*c* and *i*) and synaptophysin (*f*). VMAT1 appears predominantly at the tips of neuritic processes rather than the cell body and control serum shows no immunoreactivity (*h*). Further, VMAT1 co-localizes with secretogranin I (*c*), a marker for LDCVs. In contrast, VMAT1 staining appears distinct from synaptophysin (*f*), a marker for SLMVs. Bar, 10 μm.

center and the Golgi complex. The results account for the detection of vesicular amine transport activity in membranes prepared from the stable VMAT1 transformants even though these cells lack a known secretory compartment for regulated release such as synaptic vesicles or LDCVs. Transport activity depends on a H^+-electrochemical gradient across the vesicle membrane and several of the compartments in which the transporter apparently occurs such as the endosomes and Golgi complex contain a vacuolar H^+-ATPase that can generate such a gradient (Rudnick, 1986; Forgac, 1989).

The sorting of VMAT1 in CHO cells strongly resembles that of other synaptic vesicle proteins such as synaptophysin when they are expressed in fibroblasts (Johnston et al., 1989; Cameron et al., 1991). These observations indicate that the vesicular amine transporter contains its own signals for endocytosis. Recycling of the transporter from the cell surface after exocytotic fusion therefore does not require association with other synaptic vesicle proteins. Indeed, the expression of other synaptic vesicle proteins in CHO fibroblasts appears to result in distinct patterns of localization. In contrast to synaptophysin, synaptotagmin targets to the plasma membrane and SV2 targets to a population of vesicles that excludes the transferrin and low density lipoprotein receptors as markers of the recycling endosomal pathway (Feany et al., 1993). Interestingly, the vesicular amine transporter resembles synaptophysin more than these two other synaptic vesicle proteins in terms of targeting in CHO cells even though

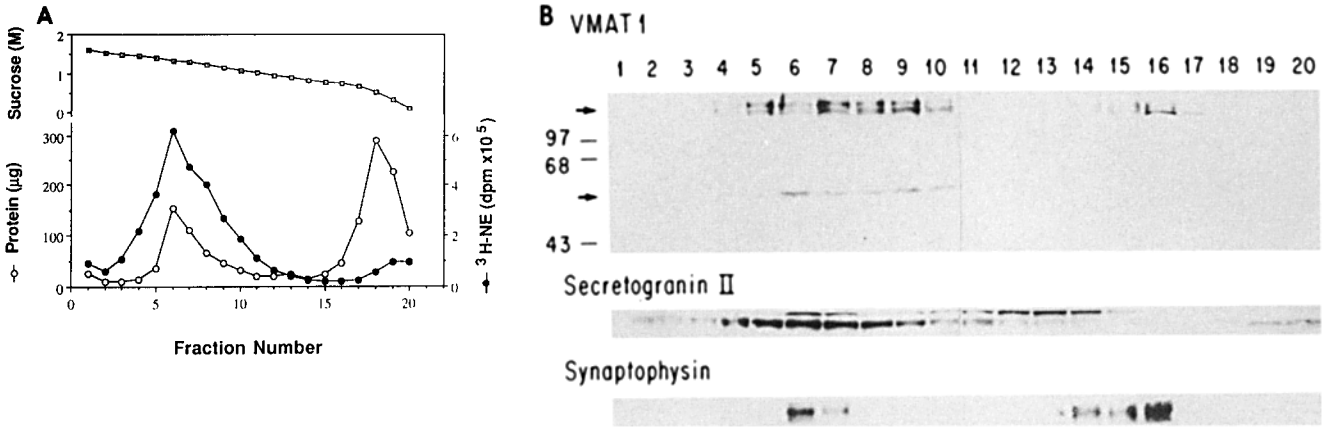

Figure 7. Distribution of VMAT1 by equilibrium sucrose density gradient fractionation of PC12 cells. PC12 cells were pre-loaded overnight with [^{3}H]norepinephrine and a postnuclear supernatant loaded onto a 0.6–1.6 M continuous sucrose gradient, with fractions collected from the bottom. (*A*) Distribution of total protein on the gradient shows two peaks, one centered at fraction 6 and the other at fraction 18. Radioactivity also accumulates in a peak centered at fraction 6 that presumably contains LDCVs. (*B*) Western blot analysis of the same fractions shown in *A* for VMAT1, secretogranin II, and synaptophysin, as described in Fig. 2. VMAT1 localizes with secretogranin to LDCVs whereas synaptophysin occurs predominantly in lighter membranes (but not soluble proteins as shown in *A*). VMAT1 occurs in two forms, the ~55-kD form also seen in CHO cells and a higher molecular weight form not seen in CHO cells. The high molecular weight form predominates in the heavier membrane fractions and is the only form seen in lighter fractions.

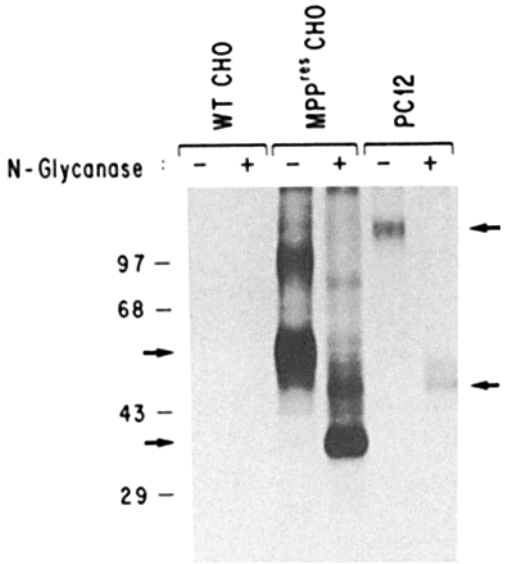

Figure 8. VMAT1 contains variable but substantial amounts of N-linked glycosylation. Wild type and transfected (*MPP^{res}*) CHO cells and PC12 cells were metabolically labeled with [^{35}S]cysteine and methionine overnight and the postnuclear supernatants immunoprecipitated with the VMAT1 antibody. The immunoprecipitates were then digested without and with N-glycanase and separated by electrophoresis as described in Fig. 2. Wild-type CHO cells contain no immunoprecipitated protein whereas stable VMAT1 transformants contain the ~55- and ~100-kD proteins seen on Western blots. Treatment with N-glycanase reduces the majority of these species to ~40 kD. The unusually high mobility of this protein both before and particularly after N-glycanase digestion presumably reflects the anomalous electrophoretic behavior of an extremely hydrophobic protein rather than degradation. In PC12 cells, the high molecular weight form predominates over a faint but detectable band at ~55 kD and is reduced to ~50 kD by N-glycanase (*arrows*).

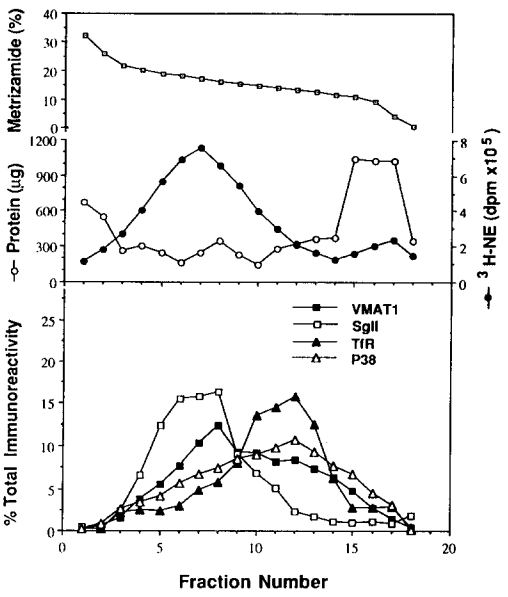

Figure 9. VMAT1 occurs predominantly on fractions corresponding to LDCVs. A post-nuclear supernatant of PC12 cells prelabeled with [^{3}H]norepinephrine was fractionated by sedimentation through metrizamide and the fractions collected from the bottom. The upper panel shows the percentage of metrizamide in each fraction and the middle panel the total protein and radioactivity in each fraction. The lower panel shows the densitometric quantitations of VMAT1, secretogranin II (*SgII*), transferrin receptor (*TfR*), and synaptophysin (*P38*) immunoreactivity from dot blots stained with the appropriate antibodies. The immunoreactivity for each of the fractions stained with one antibody was added and the percentage of the total in each fraction is shown. Secretogranin II and [^{3}H]-norepinephrine label a broad peak of LDCVs centered at fraction 7. VMAT1 labels this same broad peak but also occurs in lighter membrane fractions containing the transferrin receptor and synaptophysin as markers for endosomes and SLMVs respectively.

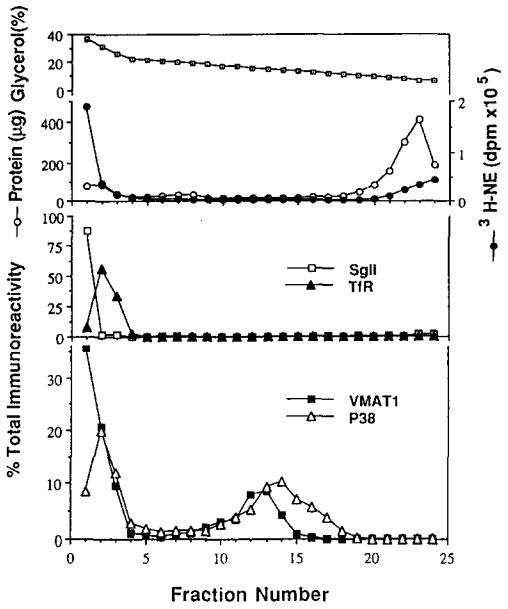

Figure 10. VMAT1 occurs on SLMVs by glycerol velocity gradient fractionation. PC12 cells were pre-labeled with [^{3}H]norepinephrine, a postnuclear supernatant sedimented through glycerol and the fractions collected from the bottom. The top panel shows the percentage of glycerol in each fraction. The middle panel shows total protein and radioactivity while the bottom panel indicates percentage of total immunoreactivity for each of the antibodies described in Fig. 9. VMAT1 roughly co-localizes with synaptophysin (*P38*) in lighter membrane fractions, indicating expression in SLMVs. VMAT1 also occurs in heavier membrane fractions that contain LDCVs as indicated by the [^{3}H]norepinephrine and secretogranin II.

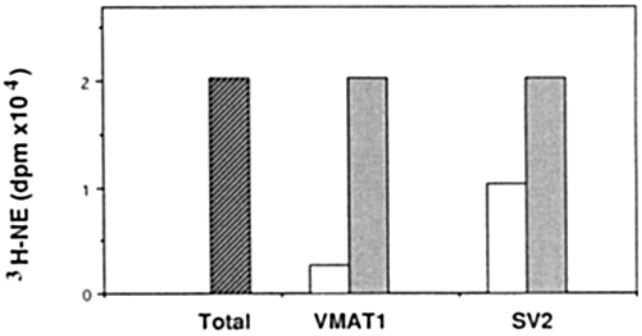

Figure 11. Immuno-isolation of pre-loaded [^{3}H]norepinephrine with the antibody to VMAT1. PC12 cells were pre-labeled with [^{3}H]norepinephrine and a post-nuclear supernatant incubated with *S. aureus* cells pre-coated with the antibody to VMAT1 and a monoclonal antibody to the vesicle proteoglycan SV2 (*stippled bars*). Both the VMAT1 and SV2 antibodies isolate all the [^{3}H]-norepinephrine pre-loaded into vesicles as measured by sedimenting all the cellular membranes at high speed (*total*). *Staphylococcus* cells pre-coated with control rabbit serum in the case of VMAT1 and control mouse serum in the case of SV2 (*open bars*) precipitated substantially less of the pre-loaded [^{3}H]norepinephrine.

sorting of the transporter and synaptophysin differ strongly in neuro-endocrine PC12 cells.

In PC12 cells, previous work using the measurement of transport activity has suggested localization of the vesicular amine transporter in LDCVs (Bauerfeind et al., 1993). We have now used an antibody to identify preferential localization of the transport protein in LDCVs both by immunofluorescence analysis of doubly stained cells and by cell fractionation using a variety of gradients. Immunoelectron microscopy of adrenal medullary cells also shows staining of chromaffin granules but the paucity of SLMVs in these cells makes it difficult to exclude a presence in that compartment as well. In addition, PC12 cells may contain more LDCVs than SLMVs but the substantial expression of other synaptic vesicle membrane proteins such as SV2 and synaptotagmin in both compartments (Buckley et al., 1985; Walch-Solimena et al., 1993) or such as synaptophysin predominantly in SLMVs (Navone et al., 1986) makes the preferential localization of the amine transporter in LDCVs unique. The biogenesis of LDCVs and synaptic vesicles differ in several important respects. LDCVs in neurons and secretory granules in endocrine cells originate from the *trans*-Golgi network (Burgess and Kelly, 1987; Trimble et al., 1991). Selected proteins such as neural peptides sort into this regulated secretory pathway through poorly characterized mechanisms. After fusion with the plasma membrane, components of the dense core granule membrane may recycle to the Golgi complex for refilling and re-release. In contrast, synaptic vesicles from neurons or SLMVs from endocrine cells appear to originate from early endosomes (Kelly, 1991). The synaptic vesicle protein synaptophysin occurs at only very low levels in dense core granules (Navone et al., 1986), suggesting that synaptic vesicles do not derive from recycled granule membrane components (Cutler and Cramer, 1990). Rather, synaptophysin travels directly to the plasma membrane in the constitutive secretory pathway and synaptic vesicles appear to bud off early endosomes (Clift-O'Grady et al., 1990; Regnier-Vigouroux et al., 1991). Thus, LDCVs derive from the regulated secretory pathway and SLMVs from the constitutive secretory pathway. The mechanism for sorting of proteins into these two pathways remains unclear. However, membrane proteins such as synaptophysin serve to distinguish SLMVs from LDCVs and may enable dissection of the relevant sorting signals. On the other hand, LDCVs contain soluble proteins and membrane-associated proteins absent from the constitutive pathway and synaptic vesicles. These proteins may sort into the regulated pathway through aggregation but a clear sorting signal has not been identified (Burgess and Kelly, 1987). However, VMAT1 now provides a clear membrane protein uniquely associated with LDCVs and not SLMVs.

In addition to neural peptides, several membrane proteins localize preferentially to LDCVs rather than to synaptic vesicles or SLMVs. These proteins include cytochrome b561 that mediates the reduction of intravesicular ascorbate, the processing enzyme peptidylglycine α-amidating monooxygenase (PAM), and dopamine β-hydroxylase (DBH). DBH does not contain a membrane-spanning domain but associates with the lumenal face of the vesicle membrane, excluding the possibility of sorting signals on the cytoplasmic surface of the vesicle. PAM occurs in two forms, one soluble and the other attached to the vesicle membrane at the COOH-terminus (Milgram et al., 1993, 1994). The two

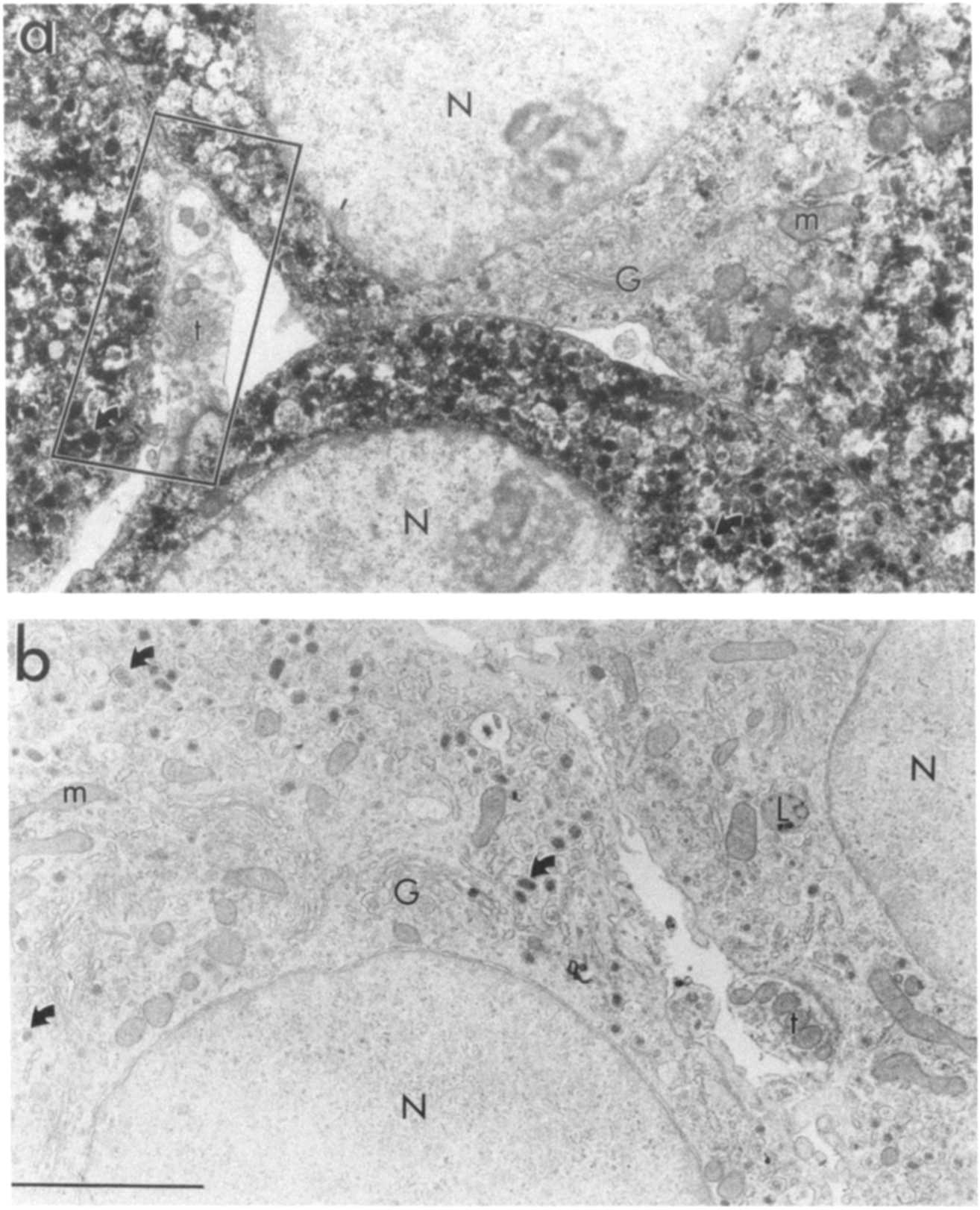

Figure 12. VMAT1 localizes to chromaffin cells exposed to the reagents for immunolabeling. Electron micrographs of chromaffin cells in the adrenal medulla (*a*) immunolabeled for VMAT1 and (*b*) not exposed to the immunoreagents. The most prominent immunolabeling in *a* occurs in chromaffin granules (*curved arrows*). Immunoreaction product is notably absent from the chromaffin cell nucleus (*N*) and from axon terminals (*t*) of adjacent neurons. In *b*, the pattern of immunolabeling seen in *a* is absent from tissue not exposed to the reagents. (*L*, lysosome; *m*, mitochondria. Bar, 2 μm.

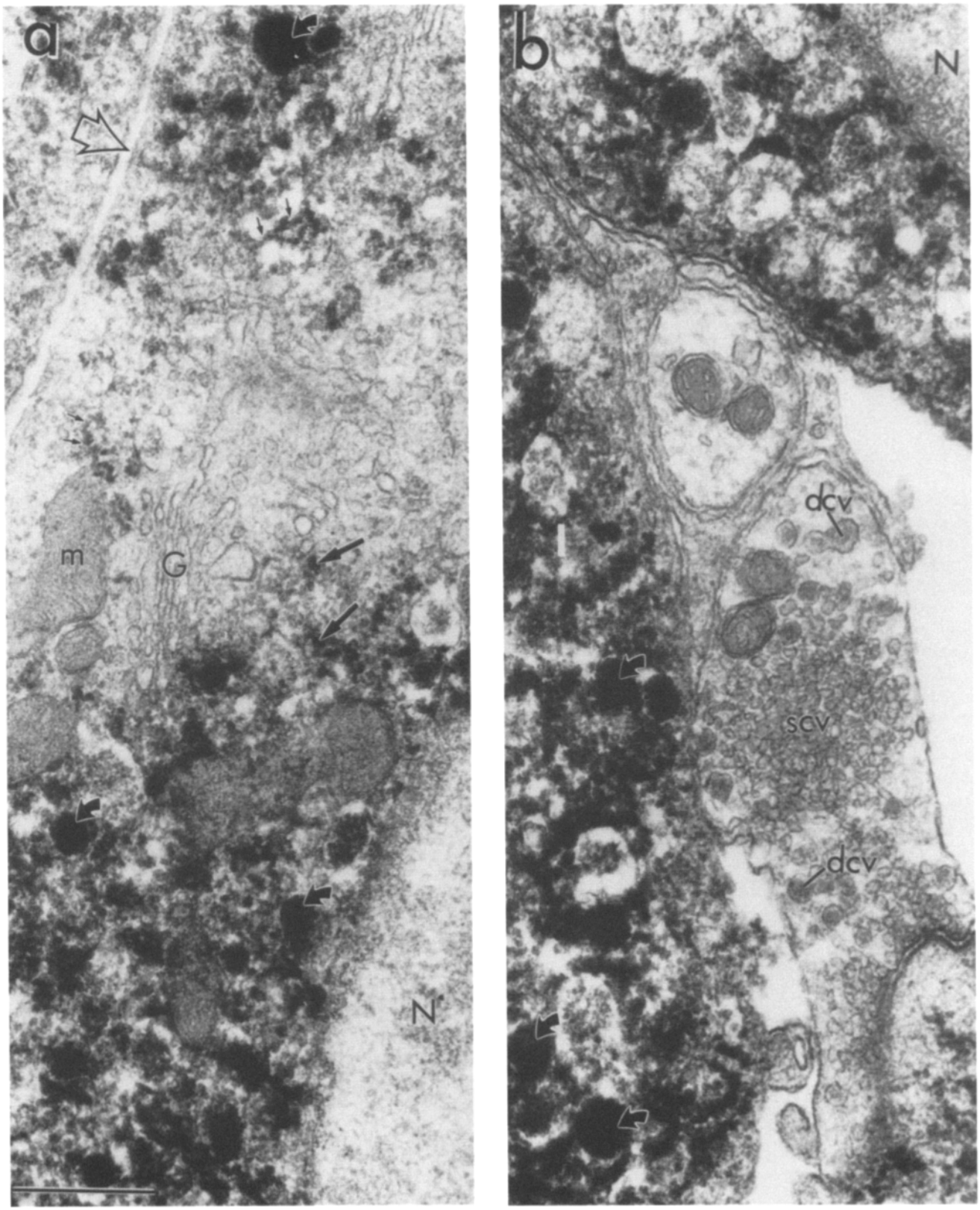

Figure 13. VMAT1 immunoreactivity localizes to chromaffin granules and not the synaptic vesicles of adjacent neuronal processes. (*a*) Electron micrograph showing immunoperoxidase reaction product for VMAT1 in most chromaffin granules (*curved arrows*). Less conspicuous labeling for VMAT1 occurs in smaller vesicles in the *trans*-Golgi network (*large arrows*) and in both endoplasmic reticulum and free polyribosomes (*small arrows*). In contrast, immunoreaction product for VMAT1 cannot be detected in mitochondria (*m*) or early Golgi apparatus (*G*). (*b*) Higher magnification electron micrograph of the boxed region in Fig. 12 *a*. Intense labeling for VMAT1 occurs in a large population of chromaffin granules (*curved arrows*), but cannot be detected in either the small clear vesicles (*scv*) or the dense core vesicles (*dcv*) of adjacent axon terminals. (*N*, nucleus of chromaffin cell; *open arrow*, outer membrane of chromaffin cell. Bar, 0.5 μm.

forms differ in their trafficking through the cell but both sort to LDCVs, indicating the importance of interactions within the interior of the vesicle for targeting to this pathway. It also remains unclear whether PAM occurs in synaptic vesicles. Cytochrome b561 has six predicted transmembrane domains (Perin et al., 1988; Kent and Fleming, 1990) and thus differs from DBH and PAM in its membrane topology. Although the cytochrome appears in both LDCVs and synaptic vesicles (Walch-Solimena et al., 1993), it is predominantly localized to the SLMV peak, suggesting that the vesicular amine transporter may be a more specific integral membrane protein for the regulated secretory pathway.

The transporter may resemble soluble proteins that are specific for LDCVs and sort into the pathway through lumenal domains. Recent evidence suggests that interactions of this type may confer sorting to the apical pathway in polarized epithelial cells (Fiedler et al., 1994). The identification of extensive N-linked glycosylation on the transporter expressed in PC12 cells but not fibroblasts further raises the possibility of interaction with lectins that may play a role in polarized targeting. However, sorting may also occur by interaction of the transmembrane and cytoplasmic domains with specific proteins of a protein sorting machinery.

Velocity gradient centrifugation through glycerol indicates that a relatively small proportion of the total vesicular amine transporter occurs in SLMVs. The small amounts of protein may account for the failure to observe vesicular amine transport activity in SLMVs prepared on sucrose density gradients, particularly when adjacent fractions containing endosomes express substantial transport activity (Bauerfeind et al., 1993). The transporter could appear in SLMVs by two distinct mechanisms. First, incomplete sorting to the regulated pathway could result in some of the transport protein reaching the cell surface through the constitutive pathway. Second, the transporter could arrive at the plasma membrane following the fusion of LDCVs. In both cases, the transporter may sort into SLMVs after endocytosis. Although the amine transporter in SLMVs represents a small fraction of the total transporter in PC12 cells, neurons in the central nervous system appear to store monoamines in small synaptic vesicles (Smith, 1972; Thureson-Klein, 1983). The identification of small amounts of the adrenal transporter in PC12 SLMVs raises the possibility that central neurons use a similar pathway to sort the transporter into synaptic vesicles. Neurons may simply increase the efficiency of sorting to this pathway. Alternatively, the vesicular amine transporter expressed in the brain may contain signals different from the adrenal transporter that increase the efficiency of this sorting.

We thank W. Huttner and P. Rosa for the generous gift of antibodies, S. Greene, and R. B. Kelly for thoughtful discussion, and B. Vigil with help in preparing the manuscript.

This research was supported by the National Institute of Mental Health, March of Dimes, and National Alliance for Research on Schizophrenia and Affective Disorders.

Received for publication 19 July 1994 and in revised form 13 September 1994.

References

Amara, S. G., and M. J. Kuhar. 1993. Neurotransmitter transporters: recent progress. *Annu. Rev. Neurosci.* 16:73–93.

Anderson, D. C., S. C. King, and S. M. Parsons. 1982. Proton gradient linkage to active uptake of ^{3}H-acetylcholine by Torpedo electric organ synaptic vesicles. *Biochemistry.* 21:3037–3043.

Andersson, P. O., S. R. Bloom, A. V. Edwards, and Jarhult. 1982. Effects of stimulation of the chorda tympani in bursts on submaxillary responses in the cat. *J. Physiol.* 322:469–483.

Bauerfeind, R., A. Regnier-Vigouroux, T. Flatmark, and W. B. Huttner. 1993. Selective storage of acetylcholine, but not catecholamines, in neuroendocrine synaptic-like microvesicles of early endosomal origin. *Neuron.* 11: 105–121.

Buckley, K., and R. B. Kelly. 1985. Identification of a transmembrane glycoprotein specific for secretory vesicles of neural and endocrine cells. *J. Cell Biol.* 100:1284–1294.

Burger, P. M., E. Mehl, P. L. Cameron, P. R. Maycox, M. Baumert, F. Lottspeich, P. De Camilli, and R. Jahn. 1989. Synaptic vesicles immunoisolated from rat cerebral cortex contain high levels of glutamate. *Neuron.* 3:715–720.

Burgess, T. L., and R. B. Kelly. 1987. Constitutive and regulated secretion of proteins. *Annu. Rev. Cell Biol.* 3:243–293.

Cameron, P. L., T. C. Sudhof, R. Jahn, and P. de Camilli. 1991. Colocalization of synaptophysin with transferrin receptors: implications for synaptic vesicle biogenesis. *J. Cell Biol.* 115:151–164.

Clift-O'Grady, L., A. D. Linstedt, A. W. Lowe, E. Grote, and R. B. Kelly. 1990. Biogenesis of synaptic vesicle-like structure in a pheochromocytoma cell line PC12. *J. Cell Biol.* 110:1693–1703.

Cutler, D. F. and L. P. Cramer. 1990. Sorting during transport to the surface of PC12 cells: divergence of synaptic vesicle and secretory proteins. *J. Cell Biol.* 110:721–730.

De Camilli, P., and R. Jahn. 1990. Pathways to regulated exocytosis in neurons. *Annu. Rev. Physiol.* 52:625–645.

Edwards, R. H. 1992. The transport of neurotransmitters into synaptic vesicles. *Curr. Opin. Neurobiol.* 2:586–594.

Edwards, R. H., M. J. Selby, W. C. Mobley, S. L. Weinrich, D. E. Hruby, and W. J. Rutter. 1988. Processing and secretion of nerve growth factor: expression in mammalian cells with a vaccinia virus vector. *Mol. Cell. Biol.* 8:2456–2464.

Erickson, J. D., L. E. Eiden, and B. J. Hoffman. 1992. Expression cloning of a reserpine-sensitive vesicular monoamine transporter. *Proc. Natl. Acad. Sci. USA.* 89:10993–10997.

Feany, M. B., A. G. Yee, M. L. Delvy, and K. M. Buckley. 1993. The synaptic vesicle proteins SV2, synaptotagmin and synaptophysin are sorted to separate cellular compartments in CHO fibroblasts. *J. Cell Biol.* 123:575–584.

Fielder, K., R. G. Parton, R. Kellner, T. Etzold, and K. Simons. 1994. VIP36, a novel component of glycolipid rafts and exocytic carrier vesicles in epithelial cells. *EMBO (Eur. Mol. Biol. Organ.) J.* 13:1729–1740.

Forgac, M. 1989. Structure and function of vacuolar class of ATP-driven proton pumps. *Physiol. Rev.* 69:765–796.

Green, S. A., H. Setiadi, R. P. McEver, and R. B. Kelly. 1994. The cytoplasmic domain of P-selectin contains a sorting determinant that mediates rapid degradation in lysosomes. *J. Cell Biol.* 124:435–448.

Harlow, E., and D. Lane. 1988. A Laboratory Manual. Cold Spring Harbor Press, Cold Spring Harbor, NY. 726 pp.

Hell, J. W., P. R. Maycox, and R. Jahn. 1990. Energy dependence and functional reconstitution of the gamma-aminobutyric acid carrier from synaptic vesicles. *J. Biol. Chem.* 265:2111–2117.

Hsu, S. M., L. Raine, and H. Fayer. 1981. The use of avidin-biotin-peroxidase complex (ABC) in immunoperoxidase technique: a comparison between ABC and unlabeled antibody (peroxidase) procedures. *J. Histochem. Cytochem.* 29:577–599.

Isambert, M. F., B. Gasnier, D. Botton, and J. P. Henry. 1992. Characterization and purification of the monoamine transporter of bovine chromaffin granules. *Biochemistry.* 31:1980–1986.

Johnson, R. G. 1988. Accumulation of biological amines into chromaffin granules: a model for hormone and neurotransmitter transport. *Physiol. Rev.* 68:232–307.

Johnston, P. A., P. L. Cameron, H. Stukenbrok, R. Jahn, P. De Camilli, and T. C. Sudhof. 1989. Synaptophysin is targeted to similar microvesicles in CHO and PC12 cells. *EMBO (Eur. Mol. Biol. Organ.) J.* 8:2863–2872.

Kanner, B. I. and S. Schuldiner. 1987. Mechanisms of storage and transport of neurotransmitters. *CRC Crit. Rev. Biochem.* 22:1–38.

Kelly, R. B. 1991. Secretory granule and synaptic vesicle formation. *Curr. Opin. Cell Biol.* 3:654–660.

Kent, U. M., and P. J. Fleming. 1990. Cytochrome b561 is fatty acylated and oriented in the chromaffin granule membrane with its carboxyl terminus cytoplasmically exposed. *J. Biol. Chem.* 265:16422–16427.

Leranth, C., and V. M. Pickel. 1989. Electron microscopic pre-embedding double immunostaining methods. *Neuroanatomical Tract-Tracing Methods, Recent Progress.* II: 129–172. L. Heimer and L. Zaborsky, editors. Plenum Publishing Corp., New York.

Liu, Y., A. Roghani, and R. H. Edwards. 1992*a*. Gene transfer of a reserpine-sensitive mechanism of resistance to MPP+. *Proc. Natl. Acad. Sci. USA.* 89:9074–9078.

Liu, Y., D. Peter, A. Roghani, S. Schuldiner, G. G. Prive, D. Eisenberg, N. Brecha, and R. H. Edwards. 1992*b*. A cDNA that suppresses MPP+ toxicity encodes a vesicular amine transporter. *Cell.* 70:539–551.

Martin, J. L., and P. J. Magistretti. 1989. Pharmacological studies of the voltage-sensitive Ca++ channels involved in the release of vasoactive intestinal peptide evoked by K+ in mouse cerebral cortical slices. *Neuroscience*. 30:423–431.

Matteoli, M., C. Haimann, F. Torri-Tarelli, J. M. Polak, B. Ceccarelli, and P. De Camilli. 1988. Differential effect of alpha-latrotoxin on exocytosis of acetylcholine-containing small synaptic vesicles and CGRP-containing large dense-core vesicles at the frog neuromuscular junction. *Proc. Natl. Acad. Sci. USA*. 85:7366–7370.

Maycox, P. R., T. Deckwerth, J. W. Hell, and R. Jahn. 1988. Glutamate uptake by brain synaptic vesicles. Energy dependence of transport and functional reconstitution in proteoliposomes. *J. Biol. Chem*. 263:15423–15428.

Milgram, S. L., R. E. Mains, and B. A. Eipper. 1993. COOH-terminal signals mediate the trafficking of a peptide processing enzyme in endocrine cells. *J. Cell Biol*. 121:23–36.

Milgram, S. L., B. A. Eipper, and R. E. Mains. 1994. Differential trafficking of soluble and integral membrane secretory granule-associated proteins. *J. Cell Biol*. 124:33–41.

Navone, F., R. Jahn, G. DiGioia, H. Stukenbrok, P. Greengard, and P. De Camilli. 1986. Protein p38: an integral membrane protein specific for small vesicles of neurons and neuroendocrine cells. *J. Cell Biol*. 103:2511–2527.

Perin, M. S., V. A. Fried, C. A. Slaughter, and T. C. Sudhof. 1988. The structure of cytochrome b561, a secretory vesicle-specific electron transport protein. *EMBO (Eur. Mol. Biol. Organ.) J*. 7:2697–2703.

Rane, S., G. G. Holz, and K. Dunlap. 1987. Dihydropyridine inhibition of neuronal calcium current and substance P release. *Pflugers Arch*. 409:361–366.

Regnier-Vigouroux, A., S. A. Tooze, and W. B. Huttner. 1991. Newly synthesized synaptophysin is transported to synaptic-like microvesicles via constitutive secretory vesicles and the plasma membrane. *EMBO (Eur. Mol. Biol. Organ.) J*. 10:3589–3601.

Rudnick, G. 1986. ATP-driven H+ pumping into intracellular organelles. *Annu. Rev. Physiol*. 48:403–413.

Schweitzer, E. S., and R. B. Kelly. 1985. Selective packaging of human growth hormone into synaptic vesicles in a rat neuronal (PC12) cell line. *J. Cell Biol*. 101:667–676.

Schweitzer, E. S., and S. Paddock. 1990. Localization of human growth hormone to a subset of cytoplasmic vesicles in transfected PC12 cells. *J. Cell Sci*. 96:375–381.

Smith, A. D. 1972. Mechanisms involved in the release of noradrenaline from sympathetic nerve. *Br. Med. Bull*. 29:123–129.

Stern-Bach, Y., N. Greenberg-Ofrath, I. Flechner, and S. Schuldiner. 1990. Identification and purification of a functional amine transporter from bovine chromaffin granules. *J. Biol. Chem*. 265:3961–3966.

Sudhof, T. C., and R. Jahn. 1991. Proteins of synaptic vesicles involved in exocytosis and membrane recycling. *Neuron*. 6:665–677.

Thureson-Klein, A. 1983. Exocytosis from large and small dense cored vesicles in noradrenergic nerve terminals. *Neuroscience*. 10:245–259.

Trimble, W. S., M. Linial, and R. H. Scheller. 1991. Cellular and molecular biology of the presynaptic nerve terminal. *Annu. Rev. Neurosci*. 14:93–122.

Vincent, M. S., and J. A. Near. 1991. Identification of a [^{3}H]dihydrotetrabenazine-binding protein from bovine adrenal medulla. *Mol. Pharmacol*. 40:889–894.

Walch-Solimena, C., K. Takei, K. L. Marek, K. Midyett, T. C. Sudhof, P. De Camilli, and R. Jahn. 1993. Synaptotagmin: a membrane constituent of neuropeptide-containing large dense-core vesicles. *J. Neurosci*. 13:3895–3903.